

Helium Ash Exhaust with Single-Null Poloidal Divertor in Doublet III

M. Shimada, M. Nagami, K. Ioki, S. Izumi, M. Maeno, H. Yokomizo, K. Shinya,
H. Yoshida, and A. Kitsunozaki

*Japan Atomic Energy Research Institute at the General Atomic Company,
General Atomic Company, San Diego, California 92138*

and

N. H. Brooks, C. L. Hsieh, and J. S. deGrassie
General Atomic Company, San Diego, California 92138

(Received 6 April 1981)

The helium ash exhaust function of a divertor has been experimentally demonstrated. Helium atoms accumulate in the divertor region as the electron density of the main plasma increases. With a helium concentration of $\sim 1.6\%$ of electron density in the main plasma, neutral helium pressure at the divertor region is as high as 1.0×10^{-4} Torr. This experiment indicates the possibility of helium ash exhaust in an α -particle-heated diverted tokamak with use of pumping ducts of a practical size.

PACS numbers: 52.55.Gb

Helium ash exhaust is one of the most important issues in thermonuclear fusion research. The α particles will, unless exhausted, dilute the fuel particles and deteriorate fusion reactivity since total particle density is limited by the maximum available β . A simple divertor was proposed for the INTOR tokamak by Shimomura *et al.*¹⁻³ Their calculation showed the helium pressure at the divertor plate to be 1×10^{-5} Torr. The pumping speed then required becomes 5×10^5 l/s, which is marginally an engineering possibility. The pumped limiter experiment by Overskei *et al.*⁴ suggests that a mechanical divertor approach might work, but no experiment has fully demonstrated this capability for a helium ash exhaust. Helium enrichment is also important from the viewpoint of tritium inventory.

We wanted to test by experiments the feasibility of using a divertor to concentrate neutral helium in divertor plasmas in Doublet III.^{5,6} Figure 1 shows the experimental setup. The diverted plasma is formed in the upper half of the Doublet III vacuum vessel. This simplified divertor has the divertor coils outside the vacuum vessel and there is no special divertor chamber or divertor throat. Helium gas is injected into the vacuum vessel from the upper port in a pulse of 5 msec duration at ~ 600 msec in the discharge. The discharge lasts for 900 msec. The amount of helium gas corresponds to a helium particle density of 1.1×10^{13} cm⁻³ if it were distributed uniformly in the plasma.

A quadrupole mass analyzer installed at the lower chamber port is used to monitor neutral-helium pressure during and after the discharge.

Ionization gauges are used to detect the total pressure (hydrogen-molecule pressure) near the main plasma and in the lower chamber. The vacuum time constants of this mass analyzer and the ionization gauges are ~ 100 msec. The density of helium ions in the main plasma is obtained with the increase of electron density \bar{n}_e with helium injection. To simulate an α -particle-heated tokamak, the measurements are made after the helium pressure reaches equilibrium levels (≥ 200 ms after the helium-gas puff). Figure 2 shows the hydrogen and the helium partial pressure as a function of density with and without divertor. For diverted discharges, both the hydrogen and helium pressure at the lower chamber are strong increasing functions of density and reach values up to 4.1×10^{-3} and 9.6×10^{-5} Torr. Figure 2 also shows that the ratio of hydrogen

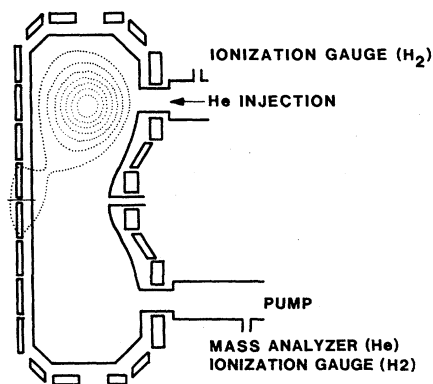


FIG. 1. Diagnostics and impurity injection system are shown with a divertor configuration with open geometry (no divertor throat, no divertor chamber, and divertor coils outside the vacuum vessel).

pressure at the lower chamber to the pressure near the main plasma increases with the increase of density and this ratio attains values up to ~ 300 at high density. On the other hand, the pressure of helium without a divertor is lower by one order of magnitude than that with a divertor. Hydrogen pressure at the lower chamber is observed to be about the same as that near the main plasma in the nondiverted discharges.

Figure 3(a) compares the increment in \bar{n}_e with helium injection for discharges with and without divertor. From this measurement, the concentration of helium ions in the main plasma (deduced as $\Delta\bar{n}_e/2$) for diverted discharges is lower than that for nondiverted discharges. For the highest density diverted discharge, the concentration of helium ions in the main plasma is $\sim 1.6\%$ of \bar{n}_e . This result shows that helium pressure of 9.6×10^{-5} Torr is attained in the lower chamber with a helium concentration of 8.2×10^{11} cm^{-3} in the main plasma. The helium compression realized in the present experiment is large enough to be applied to INTOR, where the helium allowance of 5% of \bar{n}_e ($\bar{n}_e = 1.2 \times 10^{14}$ cm^{-3}) is assumed. If we simply scale the present experimental results, a helium pressure of 7.1×10^{-4} Torr will be obtained in INTOR. The required pumping speed becomes 7.0×10^3 l/s. This value relaxes the presently proposed pumping speed

design for INTOR by a factor of 70.

There was some concern that most of the injected helium particles are directly swept out to the divertor region so that this experiment does not simulate an α -particle-heated tokamak in which helium is generated from the hot core. In order to investigate this possibility, helium gas is injected before the divertor is turned on. The helium density in the lower chamber shows no difference from the case in which helium atoms are injected after the divertor is turned on. Therefore, the experiments presented in this Letter should simulate those in an α -particle-heated plasma.

The helium enrichment is another key factor of ash exhaust from the viewpoint of tritium inventory. The helium enrichment factor, defined by

$$\eta = (P_{\text{He}}/2P_{\text{H}_2})_{\text{lower chamber}} / (n_{\text{He}}/\bar{n}_e)_{\text{main plasma}}$$

is presented in Fig. 3(b) as a function of \bar{n}_e . The helium enrichment factor is found to be almost constant for variation in \bar{n}_e , with a range of values $0.5 < \eta < 1.0$. This result shows that compression of hydrogen and helium neutrals in the lower chamber are similar. That is, neither strong helium enrichment¹⁻³ nor impoverishment⁷ is found. In nondiverted discharges η is found in the range $1.0 < \eta < 2.0$, showing a slight enrichment. It is difficult, however, to assess

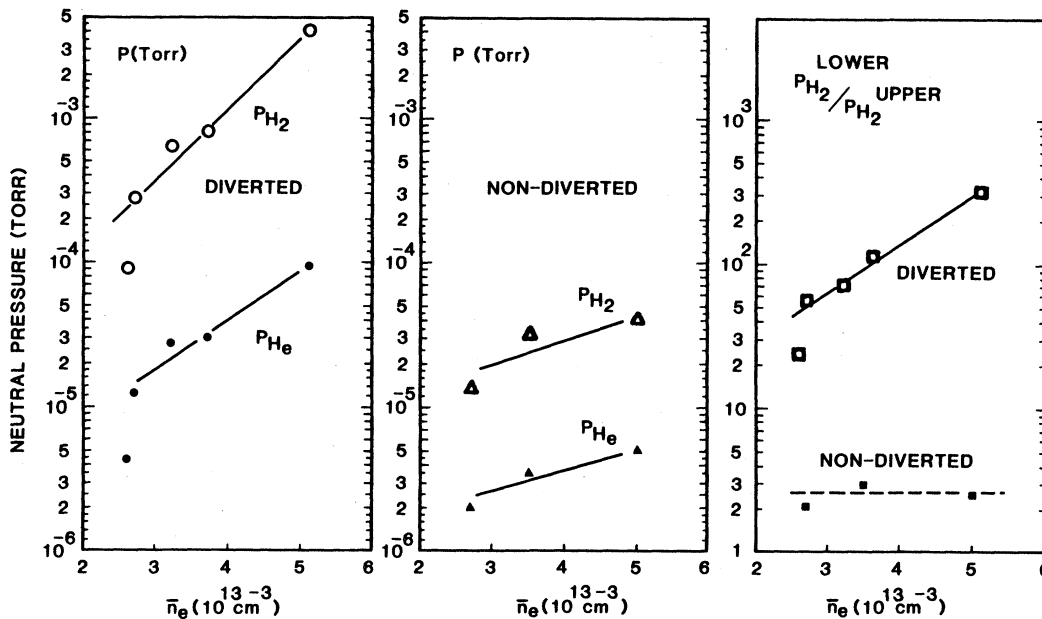


FIG. 2. Pressure of molecular hydrogen and helium measured at the lower chamber port vs electron density with and without divertor. The ratio P_{H_2} measured at the lower chamber port to P_{H_2} near the main plasma is also shown. In a high-density divertor discharge, P_{He} reaches $\sim 1 \times 10^{-4}$ Torr with a helium concentration of 1.6% in the main plasma. This result demonstrates the effective ash exhaust function of a divertor.

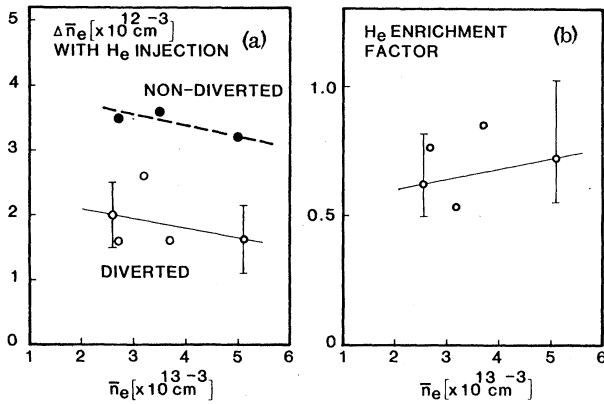


FIG. 3. (a) The increment of electron density after helium injection vs \bar{n}_e . (b) Helium enrichment factor η defined by

$$\eta = (P_{\text{He}}/2P_{\text{H}_2})_{\text{lc}} / (n_{\text{He}}/\bar{n}_e)_{\text{mp}}$$

is $0.5 < \eta < 1.0$ with divertor. (n_{He} derived by $\Delta \bar{n}_e / 2$; subscripts "lc" and "mp" denote lower chamber and main plasma, respectively.)

the feasibility of a mechanical divertor from this result since the pressure is measured far from the limiter.

The high-density diverted discharge also provides strong accumulation of plasma density and recycling at the divertor region. Figure 4 shows the line-averaged electron density \bar{n}_{e_v} measured in the vertical path, line-averaged electron density $\bar{n}_{e_{\text{DIV}}}$ measured in the horizontal path at the

divertor ($l = 67 \text{ cm}$), and the H_α emission line measured at the main plasma and divertor as a function of density. The nonlinear increase of $\bar{n}_{e_{\text{DIV}}}$ and H_α at the divertor were previously observed⁶ with the increase of density. A nonlinear increase is not observed in \bar{n}_{e_v} (viewing path located 52 cm away from the wall). The H_α line emission has a peak at 10–13 cm from the wall (observed through an H_α -selective filter by television, and Zeeman line splitting of H_α). Thus, effective path length should be $(\frac{1}{2} - \frac{1}{7})$ of 67 cm for $\bar{n}_{e_{\text{DIV}}}$ [e.g., $\bar{n}_{e_{\text{DIV}}}(l=30 \text{ cm}) = 5 \times 10^{13} \text{ cm}^{-3}$ or $\bar{n}_{e_{\text{DIV}}}(l=67 \text{ cm}) = 2 \times 10^{13} \text{ cm}^{-3}$].

This accumulation of particles and recycling resulted in strong radiative cooling at the divertor. By increasing the \bar{n}_e , the radiative power in the main plasma P_r stays almost constant around $P_r/P_O \sim (20-30)\%$, while the remote radiation in the divertor region P_{rr} increases up to $P_{rr}/P_O \sim 50\%$ (P_O is Ohmic input power). The measured maximum radiative power density is $\sim 0.3 \text{ W/cm}^3$. As a result of this strong remote cooling, electron temperature T_e is cooled to $\leq 7 \text{ eV}$ near the divertor plate. From two-dimensional television observation of the oxygen line emission at the divertor region, the electron temperature near the divertor plate is inferred to be $\sim 7 \text{ eV}$. The neutral temperature near the divertor plate is measured with Doppler broadening of the H_α line, giving $\sim 2 \text{ eV}$. Since the mean free path of

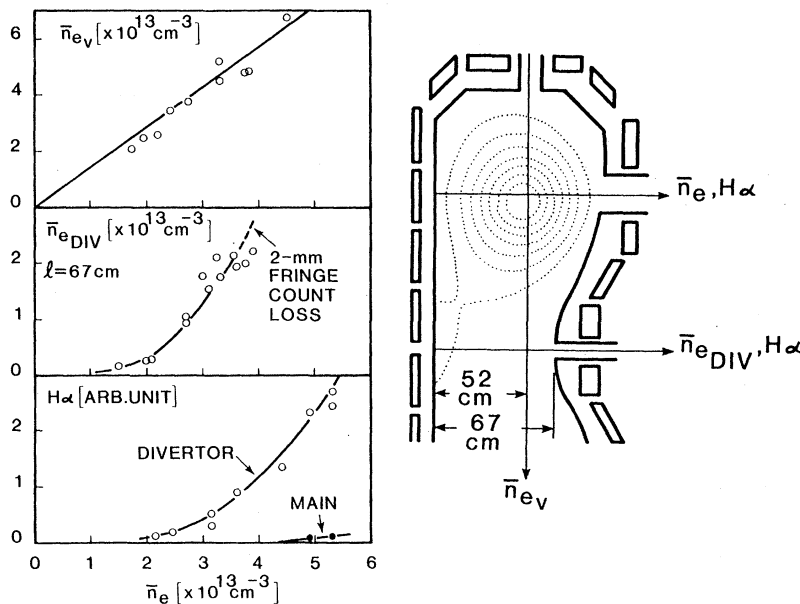


FIG. 4. Vertical average density \bar{n}_{e_v} , electron density at the divertor region ($l = 67 \text{ cm}$), and H_α line intensity along the central chord, and a chord through the divertor, vs \bar{n}_e . Nonlinear increase appears in $\bar{n}_{e_{\text{DIV}}}$ and H_α at the divertor and not in \bar{n}_{e_v} .

the charge exchange is short (< 3 cm) when $n_e > 5 \times 10^{13} \text{ cm}^{-3}$, the neutral temperature should be equilibrated with the ion temperature near the divertor plate.

A one-dimensional heat flow equation along the scrape off field line, with remote radiative cooling $P_{r\text{DIV}}$ by oxygen, was solved. The result shows a sufficient cooling of the divertor plasma. The equations are⁸

$$\nabla_{\parallel}(K_{\parallel}\nabla_{\parallel}T_e) = P_{r\text{DIV}}, \quad \nabla_{\parallel}(n_e T_e) = 0.$$

The boundary conditions of heat flow are $-(B_p/B_T)SK_{\parallel}\nabla_{\parallel}T_e = P_O - P_r$ at the main plasma, $-K_{\parallel}\nabla_{\parallel}T_e = \gamma\Gamma T_e$ at the divertor plate, where K_{\parallel} is the electron-heat-conduction coefficient for parallel flow, (B_p/B_T) is the pitch of the magnetic field, S the cross sectional area of divertor scrape off, $\gamma = 7.8$ and the particle flux $\Gamma (= 0.3 \text{ Cs } n_e)$.⁹ Computations are performed for 1% oxygen contamination of n_e , and $P_O - P_r = 300 \text{ kW}$. For the electron density at the edge of the main plasma $n_{e_b} = 1.2 \times 10^{13} \text{ cm}^{-3}$ ($\bar{n}_e \sim 5 \times 10^{13} \text{ cm}^{-3}$), the average $P_{r\text{DIV}}$ attains values $\sim 0.3 \text{ W/cm}^2$. The divertor plasma is cooled from 27 eV near the main plasma down to 1 eV at the divertor plate, while n_e near the divertor plate reaches $(0.5-5) \times 10^{14} \text{ cm}^{-3}$. If the radiation power is neglected, T_e and n_e near the divertor plate will be 12 eV and $3.1 \times 10^{19} \text{ cm}^{-3}$. In the low n_e case of $n_{e_b} = 0.4 \times 10^{13} \text{ cm}^{-3}$ ($\bar{n}_e \sim 2 \times 10^{13} \text{ cm}^{-3}$), $P_{r\text{DIV}}$ is negligible, and the T_e and n_e profiles are flat along the field line. Accordingly, the remote radiative cooling is effective in formation of the dense and cold divertor plasma.

The ionization probability of neutral helium in the divertor plasma was calculated with use of the calculated n_e and T_e profile. The result shows that 30–50% of helium neutral is ionized in the low n_e case, and greater than 90% in the high-density case. This calculation suggests that the suppression of helium backflow to the main plasma will be stronger in the high-density case, due to the shorter ionization mean free path. The frictional force exerted on the ionized helium will further suppress the backflow in the high-density case. It therefore appears that the dense and cold plasma formed by remote radiative cooling provides an effective exhaust of helium ash particles.

The conclusions are summarized as follows:

(1) Without any divertor chamber or divertor throat, neutral helium is concentrated at the divertor region with pressure up to 1.0×10^{-4} Torr with a helium concentration at 1.6% of electron density in the main plasma. No strong enrichment or impoverishment of helium is found in the divertor region.

(2) Helium pressure in the lower chamber without divertor is lower than that with divertor by one order of magnitude.

(3) Helium ash exhaust is realistic in an α -particle-heated diverted tokamak.

The authors would like to acknowledge Dr. Y. Shimomura, Dr. K. Burrell, Dr. S. Konoshima, Dr. T. Takizuka, and Dr. N. Ohyabu for their stimulating discussions. Following our experiment, helium exhaust was studied also in the expanded boundary geometry in Doublet III. We gratefully acknowledge Dr. J. DeBoo for communicating these results prior to publication and particularly for discussion of evidence indicating helium absorption on the walls. The authors would like to express their sincere gratitude to Dr. T. Ohkawa, Dr. N. Fujisawa, Dr. M. Yoshikawa, and Dr. S. Mori for their continuing encouragement throughout this work.

¹Y. Shimomura *et al.*, Japan Atomic Energy Research Institute Report No. JAERI-M8294, 1979 (unpublished).

²T. Takizuka *et al.*, in Proceedings of the Eighth International Conference on Plasma Physics and Controlled Nuclear Fusion Research, Brussels, Belgium, July 1980 (to be published), International Atomic Energy Agency Report No. CN-38/X-2-1.

³Y. Seki *et al.*, Nucl. Fusion **20**, 1213 (1980).

⁴D. Overskei *et al.*, Phys. Rev. Lett. **46**, 177 (1981).

⁵M. Nagami *et al.*, Nucl. Fusion **20**, 1325 (1980).

⁶M. Nagami *et al.*, in Proceedings of the Eighth International Conference on Plasma Physics and Controlled Nuclear Fusion Research, Brussels, Belgium, July 1980 (to be published), International Atomic Energy Agency Report No. CN-38/0-2.

⁷J. D. Callen *et al.*, in Proceedings of the Eighth International Conference on Plasma Physics and Controlled Nuclear Fusion Research, Brussels, Belgium, July 1980 (to be published), International Atomic Energy Agency Report No. CN-38/Y-3.

⁸M. A. Mahdavi *et al.*, Report No. GA-A16334, 1981 (unpublished). The reduced version of transport equation used here was first used by M. A. Mahdavi. In this reference, however, Doublet III results are explained without explicit inclusion of radiation.

⁹H. Kimura *et al.*, Nucl. Fusion **18**, 1195 (1978).